Symmetric Positive 4^{th} Order Tensors & their Estimation from Diffusion Weighted MRI

Angelos Barmpoutis[1], Bing Jian, and Baba C. Vemuri

University of Florida, Gainesville FL 32611, USA,
{abarmpou, bjian, vemuri}@cise.ufl.edu

Abstract. In Diffusion Weighted Magnetic Resonance Image (DW-MRI) processing a 2^{nd} order tensor has been commonly used to approximate the diffusivity function at each lattice point of the DW-MRI data. It is now well known that this 2^{nd}-order approximation fails to approximate complex local tissue structures, such as fibers crossings. In this paper we employ a 4^{th} order symmetric positive semi-definite (PSD) tensor approximation to represent the diffusivity function and present a novel technique to estimate these tensors from the DW-MRI data guaranteeing the PSD property. There have been several published articles in literature on higher order tensor approximations of the diffusivity function but none of them guarantee the positive semi-definite constraint, which is a fundamental constraint since negative values of the diffusivity coefficients are not meaningful. In our methods, we parameterize the 4^{th} order tensors as a sum of squares of quadratic forms by using the so called Gram matrix method from linear algebra and its relation to the Hilbert's theorem on ternary quartics. This parametric representation is then used in a nonlinear-least squares formulation to estimate the PSD tensors of order 4 from the data. We define a metric for the higher-order tensors and employ it for regularization across the lattice. Finally, performance of this model is depicted on synthetic data as well as real DW-MRI from an isolated rat hippocampus.

1 Introduction

Data processing and analysis of matrix-valued image data is becoming quite common as imaging sensor technology advances allow for the collection of matrix-valued data sets. In medical imaging, during the last decade, it has become possible to collect magnetic resonance image (MRI) data that measures the apparent diffusivity of water in tissue *in vivo*. A 2^{nd} order tensor has commonly been used to approximate the diffusivity profile at each image lattice point in a DW-MRI [4]. The approximated diffusivity function is given by

$$d(\mathbf{g}) = \mathbf{g}^T \mathbf{D} \mathbf{g} \tag{1}$$

where $\mathbf{g} = [g_1 \ g_2 \ g_3]^T$ is the magnetic field gradient direction and $\mathbf{D}$ is the estimated 2^{nd}-order tensor. This approximation yields a diffusion tensor (DT-MRI) data set $\mathbf{D}_i$, which is a 3D matrix-valued image, where subscript i denotes

location on a 3D lattice. These tensors $\mathbf{D}_i$ are elements of the space of 3×3 symmetric positive-definite matrices. Mathematically, these tensors belong to a Riemannian symmetric space, where a Riemannian metric assigns an inner product to each point of this space. Using this metric, one can perform various computations, e.g. interpolation, geodesics, geodesic PCA [3, 7, 11].

Use of higher order tensors was proposed in [9] to represent more complex diffusivity profiles which better approximate the diffusivity of the local tissue geometry. *To date however, none of the methods reported in literature for the estimation of the coefficients of higher order tensors preserve the positive definiteness of the diffusivity function.*

The use of a 4^{th}-order covariance tensor was proposed by Basser and Pajevic in [5]. This covariance tensor is employed in defining a Normal distribution of 2^{nd} order diffusion tensors. This distribution function has been employed in [6] for higher-order multivariate statistical analysis of DT-MRI datasets using spectral decomposition of the 4^{th}-order covariance matrix into eigenvalues and eigentensors (2^{nd} order). However, 2^{nd} order tensors are used to approximate the diffusivity of each lattice point of a MR dataset, failing to approximate complex local tissue structures, such as fiber crossings.

In this paper we approximate the diffusivity profile using 4^{th}-order tensors. We propose a novel parametrization of these positive-definite higher order tensors as a sum of squares of quadratic (2^{nd}-order) forms. This parametrization is enforced by employing the Gram matrix method in conjunction with the Hilbert's theorem on ternary quartics [8]. We present an efficient algorithm which estimates 4^{th}-order symmetric positive semi-definite diffusion tensors from diffusion weighted MR images. We also propose a distance measure for the space of higher-order tensors that can be computed in closed form, and employ it to regularize the estimated data across the lattice. Finally, we present experimental results using real diffusion-weighted MR data from an isolated rat hippocampus. The motivation for processing and analyzing the hippocampus lies in its important role in semantic and episodic formation, which is particularly vulnerable to acute or chronic injury [1, 15]. Based on knowledge of hippocampal anatomy, complex local tissue structures such as fiber crossings are commonly present at the anatomical regions of stratum lacunosum-moleculare, hilus, molecular layer (see fig. 3(d) region 4) and stratum lucidum (fig. 3(d) region 5). The techniques being developed here can approximate accurately such crossings and complex fiber structures and thus could prove useful in improving the sensitivity and specificity of diffusion MRI for detecting and monitoring hippocampal diseases.

The rest of the paper is organized as follows: In section 2, we present a novel parametrization of the 4^{th}-order tensors that is used to enforce the positivity semi-definiteness of the estimated tensors. In section 2.1, we present a method to estimate 4^{th}-order tensors from diffusion-weighted MR images. Furthermore, in section 2.2 we propose a distance measure for the space of 4^{th}-order tensors, and we employ it for regularization of the estimated tensor field. Section 3 contains the experimental results and comparisons with other methods using simulated

diffusion MRI data and real MR data from an isolated rat hippocampus. In section 4 we conclude.

2 Diffusion tensors of 4th order

The diffusivity function can be modeled by Eq. (1) using a 2^{nd}-order tensor. Studies have shown that this approximation fails to model complex local structures of the diffusivity in real tissues [10] and a higher-order approximation must be employed instead. A 4^{th}-order tensor can be employed in the following diffusivity function

$$d(\mathbf{g}) = \sum_{i+j+k=4} D_{i,j,k} g_1^i g_2^j g_3^k \tag{2}$$

where $\mathbf{g} = [g_1\ g_2\ g_3]^T$ is the magnetic field gradient direction. It should be noted that in the case of 4^{th}-order symmetric tensors there are 15 unique coefficients $D_{i,j,k}$, while in the case of 2^{nd}-order tensors we only have 6.

In DW-MRI the diffusivity of the water is a positive quantity. This property is essential since negative diffusion coefficients are nonphysical. However there is no guarantee that the estimated coefficients $D_{i,j,k}$ by the above process, will form a positive semi-definite tensor. Therefore, we need to develop a new parametrization of the 4^{th}-order tensor, which enforces the positive semi-definite property of the estimated tensor.

Regarding g_i in (2) as variables, the equivalence between symmetric tensors and homogeneous polynomials is straightforward. Moreover if a symmetric tensor is PSD, then its corresponding polynomial must be nonnegative for all real-valued variables. Hence here we are concerned with the positive definiteness of homogenous polynomials of degree 4 in 3 variables, or the so called *ternary quartics*. In this work we propose a novel parametrization of the symmetric 4^{th}-order PSD tensors, using the Hilbert's theorem on positive ternary quartics, was first proved by Hilbert in 1888 (see [13] for modern exposition):

Theorem 1. *Every positive real ternary quartic is a sum of three squares of quadratic forms.*

Assuming the most general case, a PSD ternary quartic can be expressed as a sum of N squares of quadratic forms as.

$$d(\mathbf{g}) = (\mathbf{v}^T\mathbf{q}_1)^2 + ... + (\mathbf{v}^T\mathbf{q}_N)^2 = \mathbf{v}^T\mathbf{Q}\mathbf{Q}^T\mathbf{v} = \mathbf{v}^T\mathbf{G}\mathbf{v} \tag{3}$$

where $\mathbf{v}$ is a properly chosen vector of monomials, (e.g. $[g_1^2\ g_2^2\ g_3^2\ g_1g_2\ g_1g_3\ g_2g_3]^T$), $\mathbf{Q} = [\mathbf{q}_1|...|\mathbf{q}_N]$ is a $6 \times N$ matrix by stacking the 6 coefficient vectors $\mathbf{q}_i$ and $\mathbf{G} = \mathbf{Q}\mathbf{Q}^T$ is the so called *Gram matrix*.

Using this Gram matrix $\mathbf{G}$ expression, Eq. (2) can be written as $d(\mathbf{g}) = \mathbf{v}^T\mathbf{G}\mathbf{v}$, and the correspondence between the 4^{th}-order tensor coefficients $D_{i,j,k}$

of Eq. (2) and the Gram matrix $\mathbf{G}$ can be established as follows:

$$\mathbf{G} = \begin{pmatrix} D_{4,0,0} & a & b & \frac{1}{2}D_{3,1,0} & \frac{1}{2}D_{3,0,1} & d \\ a & D_{0,4,0} & c & \frac{1}{2}D_{1,3,0} & e & \frac{1}{2}D_{0,3,1} \\ b & c & D_{0,0,4} & f & \frac{1}{2}D_{1,0,3} & \frac{1}{2}D_{0,1,3} \\ \frac{1}{2}D_{3,1,0} & \frac{1}{2}D_{1,3,0} & f & D_{0,2,2} - 2a & \frac{1}{2}D_{2,1,1} - d & \frac{1}{2}D_{1,2,1} - e \\ \frac{1}{2}D_{3,0,1} & e & \frac{1}{2}D_{1,0,3} & \frac{1}{2}D_{2,1,1} - d & D_{2,0,2} - 2b & \frac{1}{2}D_{1,1,2} - f \\ d & \frac{1}{2}D_{0,3,1} & \frac{1}{2}D_{0,1,3} & \frac{1}{2}D_{1,2,1} - e & \frac{1}{2}D_{1,1,2} - f & D_{0,2,2} - 2c \end{pmatrix} \quad (4)$$

where a, b, c, d, e, f are free parameters, i.e for any choice of those parameters the obtained Gram matrix represents the same 4^{th}-order tensor [12]. According to Theorem 1, if $N = 3$ (i.e. Gram matrix $\mathbf{G}$ has rank 3) then the whole space of PSD ternary quartics is spanned. For some specific choices of the parameters a, b, c, d, e, f of Eq. (4), the rank of matrix $\mathbf{G}$ becomes 3 [12]. Powers and Reznick in [12] worked on finding fundamentally different choices of those parameters that yield the same given PSD ternary quartic, i.e. in how many different ways can a ternary quartic be expressed as a sum of squares of three quadratic forms. However, given a Gram matrix $\mathbf{G}$ we can uniquely compute the coefficients $D_{i,j,k}$ of the tensor (see Eq. (4)). Therefore, we can employ the Gram matrix method for the estimation of the coefficients $D_{i,j,k}$ of the diffusion tensor from MR images using the following two steps: 1) first we estimate a Gram matrix $\mathbf{G}$ from the MR signal of the given images, and then 2) we uniquely compute the coefficients $D_{i,j,k}$ of the 4^{th}-order tensor by using formulas obtained from Eq. (4). Note that although the estimated matrix $\mathbf{G}$ is not unique, the coefficients $D_{i,j,k}$ are uniquely determined.

In the following section we will employ this Gram matrix method to enforce the positive semi-definite property of the estimated diffusion tensors from the diffusion weighted MR images.

2.1 Estimation from DWI

The coefficients $D_{i,j,k}$ of a 4^{th} order diffusion tensor can be estimated from diffusion-weighted MR images by minimizing the following cost function:

$$E(\mathbf{Q}, S_0) = \sum_{i=1}^{M} (S_i - S_0 e^{-b_i \mathbf{v}_i^T \mathbf{Q}\mathbf{Q}^T \mathbf{v}_i})^2 \quad (5)$$

where M is the number of the diffusion weighted images associated with gradient vectors $\mathbf{g}_i$ and b-values b_i; S_i is the corresponding acquired signal and S_0 is the zero gradient signal. Using the magnetic field gradient directions $\mathbf{g}_i$ we construct the 6-dimensional vectors $\mathbf{v}_i = [g_{i1}^2 \; g_{i2}^2 \; g_{i3}^2 \; g_{i1}g_{i2} \; g_{i1}g_{i3} \; g_{i2}g_{i3}]^T$. In Eq. (5), the 4^{th} order diffusion tensor is parameterized using the Gram matrix $\mathbf{G} = \mathbf{Q}\mathbf{Q}^T$, where $\mathbf{Q}$ is a $6 \times N$ matrix and $N \geq 3$ is a predefined constant. In our experiments we used $N = 3$, which is justified by Theorem 1. Having estimated the matrix $\mathbf{Q}$ that minimizes Eq. (5), the coefficients $D_{i,j,k}$ can be computed directly from the Gram matrix using the relation described by the matrix of Eq. (4). S_0 can

either be assumed to be known or estimated simultaneously with the coefficients $D_{i,j,k}$ by minimizing Eq. (5).

Starting with an initial guess for S_0 and $\mathbf{Q}$, we can use any optimization method in order to minimize Eq. (5). For the optimization schemes that employ the gradients of Eq. (5) with respect to the unknown coefficients of $\mathbf{Q}$, the gradient is given by the following equation

$$\nabla_{\mathbf{Q}} E(\mathbf{Q}, S_0) = 4 \sum_{i=1}^{M} b_i S_0 e^{-b_i \mathbf{v}_i^T \mathbf{Q}\mathbf{Q}^T \mathbf{v}_i} (S_i - S_0 e^{-b_i \mathbf{v}_i^T \mathbf{Q}\mathbf{Q}^T \mathbf{v}_i}) \mathbf{v}_i^T \mathbf{v}_i \mathbf{Q} \quad (6)$$

Now given $\mathbf{Q}$ at each iteration of the optimization algorithm we can update S_0 by again minimizing Eq. (5). The derivative of this equation with respect to the unknown S_0 is

$$\nabla_{S_0} E(\mathbf{Q}, S_0) = -2 \sum_{i=1}^{M} (S_i - S_0 e^{-b_i \mathbf{v}_i^T \mathbf{Q}\mathbf{Q}^T \mathbf{v}_i}) e^{-b_i \mathbf{v}_i^T \mathbf{Q}\mathbf{Q}^T \mathbf{v}_i} \quad (7)$$

By setting Eq. (7) equal to zero, we derive the following update formula for S_0

$$S_0 = \sum_{i=1}^{M} S_i e^{-b_i \mathbf{v}_i^T \mathbf{Q}\mathbf{Q}^T \mathbf{v}_i} / \sum_{i=1}^{M} e^{-2 b_i \mathbf{v}_i^T \mathbf{Q}\mathbf{Q}^T \mathbf{v}_i} \quad (8)$$

In our experiments we used the well known Lavenberg-Marquardt (LM) nonlinear least-squares method, which has advantages over other optimization methods, in terms of stability and computational burden.

As pointed out earlier, although the coefficients $D_{i,j,k}$ are uniquely estimated, the Gram matrix parametrization $\mathbf{G} = \mathbf{Q}\mathbf{Q}^T$ is not unique, i.e. there exist different matrices $\mathbf{Q}$ which parameterize the same Gram matrix. For example there are infinitely many matrices $\mathbf{Q}$ that yield the same $\mathbf{G}$, due to the orthogonality property ($\mathbf{R}\mathbf{R}^T = \mathbf{I}$) of the rotation matrices $\mathbf{R}$, where $\mathbf{I}$ is the identity matrix. Thus, in the case that $\mathbf{Q}$ is of size 6×3, for any 3×3 orthogonal matrix $\mathbf{R}$ we have $(\mathbf{Q}\mathbf{R})(\mathbf{Q}\mathbf{R})^T = \mathbf{Q}\mathbf{Q}^T$. In order to reduce this infinite solution space to a finite set of solutions, which theoretically can be handled by the optimization techniques, we use the well known QR decomposition of real square matrices to uniquely decompose any given 6×3 matrix $\mathbf{Q}$ in the form $\mathbf{Q} = \begin{bmatrix} \mathbf{T}\mathbf{R} \\ \mathbf{A} \end{bmatrix}$, where all matrices are of size 3×3 and specifically $\mathbf{T}$ is lower triangular, and $\mathbf{R}$ is an orthogonal matrix. Then by setting $\mathbf{R} = \mathbf{I}$ we reformulate $\mathbf{Q}$ as $\mathbf{Q} = \begin{bmatrix} \mathbf{T} \\ \mathbf{A} \end{bmatrix}$ and thus the infinitely non-unique issue is replaced by a countably non-uniqueness issue, which can be handled by the optimization algorithm. Note that using this formulation there are only 15 unknown parameters in matrix $\mathbf{Q}$, which is equal to the number of the unknown coefficients $D_{i,j,k}$ of the estimated tensor.

2.2 Distance measure

In the previous section we discussed about estimating PSD 4^{th}-order tensors from DW-MRI data. For the estimation, we minimize the energy function expressed

in Eq.(5). We can add a regularization term in this energy function, in order to perform smoothing of the estimated tensors across the lattice in the DW-MRI data set. The regularization term is given by

$$\sum_j \sum_{i \in \eta_j} dist(\mathbf{D}_j, \mathbf{D}_i)^2 \tag{9}$$

where η_j is the set of lattice indices whose distance from lattice index 'j' is 1. In the regularization term defined in Eq. (9) we need to employ an appropriate distance measure between the tensors $\mathbf{D}_i$ and $\mathbf{D}_j$. Here we use the notation $\mathbf{D}$ in order to denote the set of 15 unique coefficients $D_{i,j,k}$ of a 4^{th}-order tensor.

We can define a distance measure between the 4^{th}-order diffusion tensors $\mathbf{D}_1$ and $\mathbf{D}_2$ by computing the normalized L_2 distance between the corresponding diffusivity functions $d_1(\mathbf{g})$ and $d_2(\mathbf{g})$ leading to the equation,

$$dist(\mathbf{D}_1, \mathbf{D}_2)^2 = \frac{1}{4\pi} \int_{S^2} [d_1(\mathbf{g}) - d_2(\mathbf{g})]^2 d\mathbf{g} \tag{10}$$

$$\begin{aligned}
= \frac{1}{315}[&(\Delta_{4,0,0} + \Delta_{0,4,0} + \Delta_{0,0,4} + \Delta_{2,2,0} + \Delta_{0,2,2} + \Delta_{2,0,2})^2 + \\
&4[(\Delta_{4,0,0} + \Delta_{2,2,0})^2 + (\Delta_{4,0,0} + \Delta_{2,0,2})^2 + (\Delta_{0,4,0} + \Delta_{2,2,0})^2 + \\
&(\Delta_{0,4,0} + \Delta_{0,2,2})^2 + (\Delta_{0,0,4} + \Delta_{0,2,2})^2 + (\Delta_{0,0,4} + \Delta_{2,0,2})^2] + \\
&23(\Delta_{4,0,0}^2 + \Delta_{0,4,0}^2 + \Delta_{0,0,4}^2) - 6(\Delta_{2,2,0}^2 + \Delta_{0,2,2}^2 + \Delta_{2,0,2}^2) + \\
&2(\Delta_{4,0,0} + \Delta_{0,4,0} + \Delta_{0,0,4})^2 + (\Delta_{2,1,1} + \Delta_{0,3,1} + \Delta_{0,1,3})^2 + \\
&(\Delta_{1,2,1} + \Delta_{3,0,1} + \Delta_{1,0,3})^2 + (\Delta_{1,1,2} + \Delta_{3,1,0} + \Delta_{1,3,0})^2 + \\
2\,&\left[(\Delta_{3,1,0} + \Delta_{1,3,0})^2 + (\Delta_{3,0,1} + \Delta_{1,0,3})^2 + (\Delta_{0,3,1} + \Delta_{0,1,3})^2\right] + \\
&2(\Delta_{3,1,0}^2 + \Delta_{3,0,1}^2 + \Delta_{1,3,0}^2 + \Delta_{0,3,1}^2 + \Delta_{1,0,3}^2 + \Delta_{0,1,3}^2)]
\end{aligned}$$

where, the integral of Eq. (10) is over all unit vectors $\mathbf{g}$, i.e., the unit sphere S^2 and the coefficients $\Delta_{i,j,k}$ are computed by subtracting the coefficients of the tensor $\mathbf{D}_1$ from the corresponding coefficients of the tensor $\mathbf{D}_2$.

As shown above, the integral of Eq. (10) can be computed analytically and the result can be expressed as a sum of squares of the terms $\Delta_{i,j,k}$. In this simple form, this distance measure between 4^{th}-order tensors can be implemented very efficiently. Note that this distance measure is invariant to rotations in 3-dimensional space since it was defined as an integral over all directions $\mathbf{g}$.

Another property of the above distance measure is that the average element (mean tensor) $\hat{\mathbf{D}}$ of a set of N tensors $\mathbf{D}_i$, $i = 1 \ldots N$ is defined as the Euclidean average of the corresponding coefficients of the tensors. This property can be proved by verifying that $\hat{\mathbf{D}}$ minimizes the sum of squares of distances $\sum dist(\mathbf{D}, \mathbf{D}_i)^2$. Similarly, it can be shown that geodesics (shortest paths) between 4^{th}-order tensors are defined as Euclidean geodesics.

3 Experimental results

In this section we present experimental results on our method applied to simulated DW-MRI data as well as real DW-MRI data from an isolated rat hippocampus.

In order to motivate the need of the PSD constraint in the 4^{th}-order estimation process, we performed the following experiment using a synthetic dataset. The synthetic data was generated by simulating the MR signal from a single fiber using the realistic diffusion MR simulation model in [14]. Then, we added different amounts of Riccian noise to the simulated dataset and we estimated the 4^{th}-order tensors from the noisy data by: a) minimizing $\sum_{i=1}^{M}(S_i - S_0 exp(-b_i d(\mathbf{g}_i)))^2$ without using the proposed parametrization to enforce PSD constraint and b) our method, which guarantees the PSD property of the tensors. (S_i is the MR signal of the i^{th} image and S_0 is the zero-gradient signal).

It is known that the estimated 4^{th}-order tensors represent more complex diffusivity profiles with multiple fiber orientations which better approximate the diffusivity of the local tissue geometry compared to the traditional 2^{nd}-order tensors [9]. Studies on estimating fiber orientations from the diffusivity profile have shown that the peaks of the diffusivity profile do not necessarily yield the orientations of the distinct fiber bundles [10]. One should instead employ the displacement probability profiles . The displacement probability $P(\mathbf{R})$ is given by the Fourier integral $P(\mathbf{R}) = \int E(\mathbf{q}) exp(-2\pi i \mathbf{q}\cdot\mathbf{R}) d\mathbf{q}$ where $\mathbf{q}$ is the reciprocal space vector, $E(\mathbf{q})$ is the signal value associated with vector $\mathbf{q}$ divided by the zero gradient signal and $\mathbf{R}$ is the displacement vector. In our experiments, we numerically estimated the displacement probability profiles from the 4^{th}-order tensors.

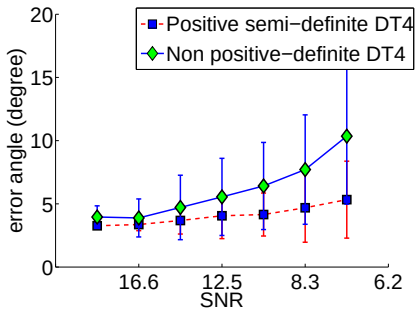

Fig. 1. Comparison of the fiber orientation errors for different amount of noise in the data, obtained by using: a) our parametrization to enforce positivity (red) and b) without enforcing positivity of the estimated tensors (in blue).

Then, we computed the displacement probability profiles of the 4^{th}-order tensors estimated earlier with the two different methods, and we computed the

fiber orientations from the maxima of the probability profiles. The error angles (mean and standard deviation) of the two methods for different amount of noise in the data are plotted in Fig. 1. As expected, our method yields smaller errors in comparison with the method that does not enforces the PSD property of the tensors. When we increase the amount of noise in the data, the errors observed by the later method are significantly increased, while our proposed method shows clearly much smaller errors. This conclusively demonstrates the need for enforcing the PSD property of the estimated tensors and validates the accuracy of our proposed method.

Furthermore, in order to compare our proposed method with other existing techniques that do not employ 4^{th}-order tensors, we performed an other experiment using synthetic data. The data were generated for different amounts of noise by following the same method as previously using the simulated MR signal of a 2-fiber crossing (see Fig. 2(a)) . We estimated 4^{th}-order tensors from the corrupted simulated MR signal using our method and then we computed the fiber orientations from the corresponding probability profiles. For comparison we also estimated the fiber orientations using the DOT method described in [10] and the ODF method presented in [2]. For all three methods we computed the estimated fiber orientation errors for different amount of noise in the data (shown in Fig. 2(b)). The results conclusively demonstrate the accuracy of our method, showing small fiber orientation errors ($\sim 6^o$) for typical amount of noise with signal to noise ratios (SNR): 12.5-16.6. Furthermore, by observing the plot, we also conclude that the accuracy of our proposed method is very close to that of the DOT method and is significantly better than the ODF method.

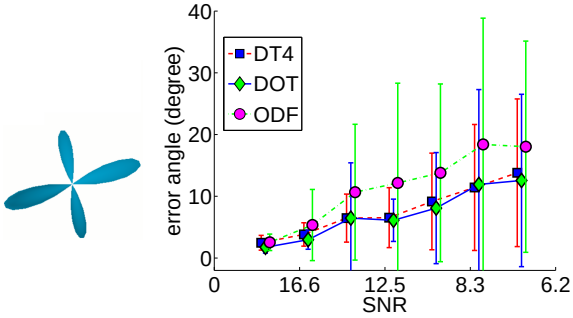

(a) (b)

Fig. 2. Fiber orientation errors for different SNR in the data using our method for the estimation of positive 4^{th}-order tensors and two other existing methods: 1) DOT and 2) ODF. In the experiment we used simulated MR signal of a 2-fiber crossing, whose probability profile is shown in (a).

In the following experiments, we used MR data from an isolated rat hippocampus. The diffusion weighted MR images of this dataset were acquired using the following protocol. This protocol included acquisition of 22 images using a pulsed gradient spin echo pulse sequence with repetition time (TR) = 1.5 s, echo time (TE) = 28.3 ms, bandwidth = 35 kHz, field-of-view (FOV) = 4.5×4.5 mm, matrix = 90×90 with 56 continuous 200-μm-thick axial slices (oriented transverse to the septo-temporal axis of the isolated hippocampus). After the first image set was collected without diffusion weighting (b $\sim$ 0 s/mm^2), 21 diffusion-weighted image sets with gradient strength (G) = 415 mT/m, gradient duration (δ) = 2.4 ms, gradient separation (Δ) = 17.8 ms and diffusion time (T_δ) = 17 ms were collected. Each of these image sets used different diffusion gradients (with approximate b values of 1250 s/mm^2) whose orientations were determined from the 2^{nd} order tessellation of an icosahedron projected onto the surface of a unit hemisphere. The image without diffusion weighting had 36 signal averages (time = 81 min), and each diffusion-weighted image had 12 averages (time = 27 min per diffusion gradient orientation) to give a total imaging time of 10.8 h per hippocampus. Temperature was maintained at 20 $\pm$ 0.2^{o}C throughout the experiments using the temperature control unit of the magnet previously calibrated by methanol spectroscopy. Figures 3(a) and 3(b) show the S_0 image and the FA map respectively of a slice extracted from the 3D volume of the above dataset.

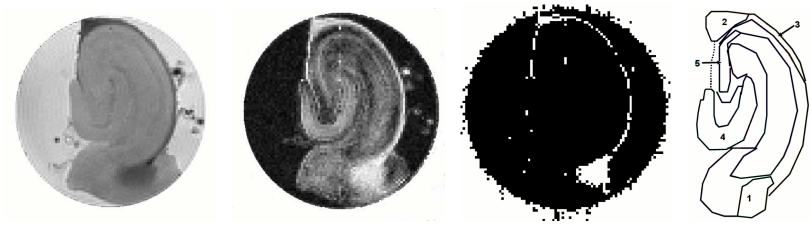

(a) (b) (c) (d)

Fig. 3. Isolated rat hipppocampus. a) S_0, b) FA, c) White pixels indicate locations where the estimated 4^{th}-order tensor was not positive-definite, d) Manually labeled image based on knowledge of hippocampal anatomy. The index of the labels is: 1) dorsal hippocampal commissure, 2) fimbria, 3) alveus, 4) molecular layer, 5) mixture of CA3 stratum pyramidale and stratum lucidum.

First, we estimated a 4^{th}-order diffusion tensor field from this dataset by minimizing $\sum_{i=1}^{M}(S_i - S_0 exp(-b_i d(\mathbf{g}_i)))^2$ without using the proposed parametrization to enforce positivity. As expected, some of the estimated tensors were not positive. In Fig. 3(c) we show in white color the locations where those non-positive-definite tensors were estimated. These tensors are mainly located in the

regions “dorsal hippocampal commissure”, “fimbria” and “alevus”, which correspond to the regions 1, 2 and 3 respectively, shown in Fig. 3(d). Based on knowledge of hippocampal anatomy, those regions are highly anisotropic with FA ~ 0.9. Therefore, from the experimental results (Fig. 3(c)) we conclude that highly anisotropic diffusivities are most likely to be inaccurately approximated by a non-positive semi-definite tensor. Thus one needs to employ a method that guarantees the PSD property.

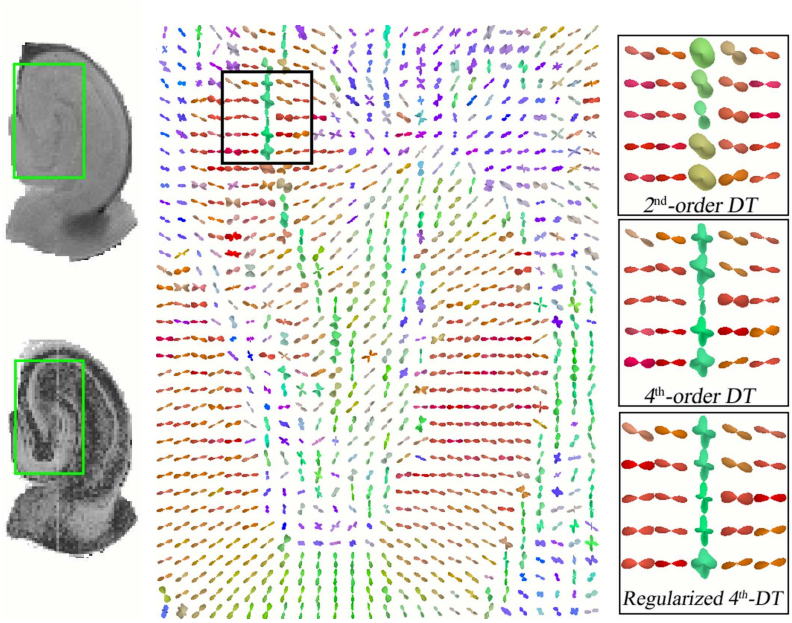

(a) (b) (c)

Fig. 4. The estimated 4^{th}-order tensor field from an isolated rat hippocampus dataset using our method. (a) top:S_0 and bottom:FA, (b) the estimated displacement probability profiles of the 4^{th}-order tensor field in the region of interest (ROI) indicated by a green rectangle in (a). (c)Comparison of the estimated 2^{nd}-order tensors (top)and the estimated probability profiles of the 4^{th}-order tensors without (middle) and with regularization (bottom) in a ROI indicated by a black rectangle in (b).

We computed the displacement probability profiles from: a) the 4^{th}-order tensor field estimated previously without the positive-definite constraint, and b) the 4^{th}-order tensor field estimated by our proposed method. In order to compare the results of the above algorithms, in Fig. 5 we plot the corresponding probability profiles from a region of interest in the “dorsal hippocampal commissure”. By observing this figure, we can say that the field of probability profiles is noisy

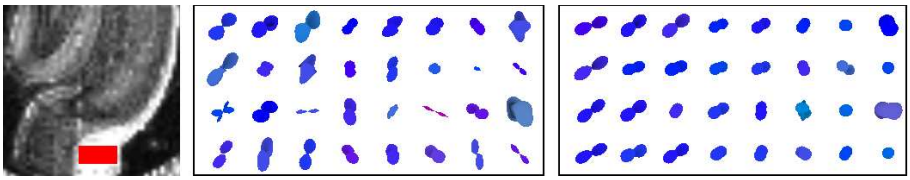

Fig. 5. Left: The region of interest from the "dorsal hippocampal commissure", which is magnified in the next plates of this figure. Comparison between the displacement probability profiles computed from non-PSD 4^{th}-order tensors (middle) and PSD tensors estimated by our method (right).

if we do not enforce the PSD constraint (Fig. 5 middle). On the other hand the profiles obtained by our method (Fig. 5 right) are more coherent and smooth. Note that this is a result of enforcing the PSD constraint, since in this experiment we did use any regularization. This demonstrates the superior performance of our algorithm and motivates the use of the proposed PSD constraint.

Finally Fig. 4(b) shows displacement probability profiles computed from the estimated (by our method) 4^{th}-order tensor field in another region of hippocampus. This tensor field corresponds to the region of interest denoted by a green rectangle in S_0 and FA map shown in Fig. 4a. The X, Y, Z components of the dominant orientation of each profile are assigned to R, G, B (red, green, blue) components of the color of each surface. By observing Fig. 4(b) we can see several fiber crossings in different regions of the rat hippocampus. One of those regions is marked by a black rectangle and it is presented enlarged in Fig. 4(c). This region is consisted of a mixture of CA3 stratum pyramidale and stratum lucidum, and it is most likely to contain fiber-crossings. As expected, in the center of this region there are profiles presenting fiber crossings. These fiber crossings cannot be resolved by using 2^{nd}-order diffusion tensors estimated from the same dataset (shown on the top of Fig. 4(c)). Finally in the bottom plate of Fig. 4(c), we show an example using the regularization term defined in section 2.2. By comparing the probability profiles shown in this image with those of the middle plate of Fig. 4(c) we can see that the regularization of the estimated data removes some of the noise in the dataset, and as a consequence some of the crossings are observed more clearly (see at the center of the image).

4 Conclusions

In diffusion weighted MR imaging 2^{nd}-order tensors have commonly been used to approximate the diffusivity profile. However, this approximation fails to represent complex local tissue structures, such as fiber crossings. 4^{th}-order tensors were employed in this work, showing better approximation capabilities compared to the 2^{nd}-order case. We presented a method for estimating the coefficients of 4^{th}-order tensors from diffusion-weighted MR images. Our technique guarantees the positive semi-definite property of the estimated tensors, which is the main

contribution of our work. This property is essential since non-PSD diffusivity profiles are not meaningful from the point of view of physics of diffusion. To date, there is no other reported work in literature which handles this constraint for rank-4 tensors. We applied our proposed algorithm to a real MR dataset from an isolated rat hippocampus. The superior performance of our method in the experimental results demonstrates the need for employing the constraint and motivates the use of our technique. The accuracy of our model was validated by using simulated MR data of fiber crossings, and compared to other existing methods. In our future work we plan to employ the methods proposed here to extend various techniques used for the 2^{nd}-order tensor fields such as segmentation, registration and fiber-tracking, to the space of higher-order tensors.

References

1. D. Amaral and M. Witter. Hippocampal formation. In *The Rat Nervous System*, pages 443–493. Academic Press, 1995.
2. A. W. Anderson. Measurement of fiber orientation distributions using high angular resolution diffusion imaging. *Magn. Reson. Med.*, 54(5):1194–1206, 2005.
3. A. Barmpoutis, B. C. Vemuri, and J. R. Forder. Robust tensor splines for approximation of Diffusion Tensor MRI data. *In Proceedings of MMBIA06*, pages 86–86, 17-18 June 2006.
4. P. J. Basser, J. Mattiello, and D. Lebihan. Estimation of the Effective Self-Diffusion Tensor from the NMR Spin Echo. *J. Magn. Reson. B*, 103:247–254, 1994.
5. P. J. Basser and S. Pajevic. A normal distribution for tensor-valued random variables: Applications to diffusion tensor MRI. *IEEE Trans. on Medical Imaging*, 22:785–794, 2003.
6. P. J. Basser and S. Pajevic. Spectral decomposition of a 4th-order covariance tensor: Applications to diffusion tensor MRI. *Signal Processing*, 87:220–236, 2007.
7. P. Fletcher and S. Joshi. Principal geodesic analysis on symmetric spaces: Statistics of diffusion tensors. *Proc. of CVAMIA*, pages 87–98, 2004.
8. D. Hilbert. Über die darstellung definiter formen als summe von formenquadraten. *Math. Ann.*, 32:342–350, 1888.
9. E. Özarslan and T. H. Mareci. Generalized diffusion tensor imaging and analytical relationships between diffusion tensor imaging and high angular resolution diffusion imaging. *Magn. Reson. Med.*, 50(5):955–965, 2003.
10. E. Özarslan, T. M. Shepherd, B. C. Vemuri, S. J. Blackband, and T. H. Mareci. Resolution of complex tissue microarchitecture using the diffusion orientation transform (DOT). *NeuroImage*, 31:1086–1103, 2006.
11. X. Pennec, P. Fillard, and N. Ayache. A Riemannian framework for tensor computing. *International Journal of Computer Vision*, 65, 2005.
12. V. Powers and B. Reznick. Notes towards a constructive proof of Hilbert's theorem on ternary quartics. In *Quadratic Forms and Their Applications (Dublin, 1999), Contemp. Math. 272, Am. Math. Soc., Providence, RI*, pages 209–227, 2000.
13. W. Rudin. Sums of squares of polynomials. *Am. Math. Monthly*, 107:813–821, 2000.
14. O. Söderman and B. Jönsson. Restricted diffusion in cylindrical geometry. *J. Magn. Reson.*, A (117):94–97, 1995.
15. L. Squire, C. Stark, and R. Clark. The medial temporal lobe. *Annu. Rev. Neurosci.*, 27:279–306, 2004.